

Novel face-detection method under various environments

Min-Quan Jing

Ling-Hwei Chen

National Chiao Tung University
Department of Computer Science
1001 Ta Hsueh Road
Hsinchu, Taiwan 30010
Republic of China
E-mail: lhchen@cc.nctu.edu.tw

Abstract. We propose a method to detect a face with different poses under various environments. On the basis of skin color information, skin regions are first extracted from an input image. Next, the shoulder part is cut out by using shape information and the head part is then identified as a face candidate. For a face candidate, a set of geometric features is applied to determine if it is a profile face. If not, then a set of eyelike rectangles extracted from the face candidate and the lighting distribution are used to determine if the face candidate is a nonprofile face. Experimental results show that the proposed method is robust under a wide range of lighting conditions, different poses, and races. The detection rate for the HHI face database is 93.68%. For the Champion face database, the detection rate is 95.15%. © 2009 Society of Photo-Optical Instrumentation Engineers. [DOI: 10.1117/1.3156843]

Subject terms: face detection; profile face; various lighting environments; skin color.

Paper 080858R received Nov. 2, 2008; revised manuscript received Mar. 22, 2009; accepted for publication Apr. 20, 2009; published online Jun. 24, 2009.

1 Introduction

Detecting a face from an image is the first step for face applications. Although it has been studied for many years, detecting a face under various environments is still challenging work. Some factors make face detection difficult. One is the variety of colored lighting sources; another is that facial features such as eyes may be partially or wholly occluded by a shadow generated by a bias lighting direction; and others are race and different face poses with/without glasses. Several methods¹⁻¹¹ had been proposed to detect faces. Some²⁻⁴ use eigenface, neural network, and support vector machine to detect faces of restricted poses under normal lighting condition. Hsu et al.⁵ proposed a face detection algorithm that uses a nonlinear transform to overcome the variance of the skin tones. Some defined chroma properties are used to extract the facial features and applied to verify a face. Chow et al.⁶ proposed an approach to locate a face candidate under different lighting conditions and then applied an eigenmask-based method to verify the face. However, these methods failed to locate faces with some kinds of poses (such as a near-profile and profile face). Shih and Chuang⁷ used shape and contour information to locate a face in a plain background and normal lighting condition. However, it is difficult to detect a face in a complex background and various lighting conditions. Wu and Zhou⁸ proposed an algorithm to locate face candidates using eye-analog segment information. The algorithm would fail when a person wears glasses. Some methods⁹⁻¹¹ use mosaic, edge, and mathematical morphology to detect eyes; however, these methods would fail to locate eyes when a face is under poor lighting conditions (such as a bias light source). As mentioned above, various lighting conditions, different head poses, glasses, race, and complex

backgrounds are factors that make face detection difficult. To solve these problems, we propose a method to detect a face with/without eyeglasses under various poses and environments. Figure 1 shows the block diagram of the proposed face detector. First, we use skin color to extract candidate skin regions. Next, shape information is used to judge whether a skin region contains a shoulder part. If it does, then a skin-projection-based method is applied to remove it and the head part is labeled as a face candidate for further processing. For each face candidate, a set of geometric constraints are first applied to judge if the face candidate is a profile face. If not, some eyelike rectangles (ERs) are first extracted. Then, based on these ERs, a horizontal eye line and a vertical symmetric line are located to judge if the face candidate is a nonprofile face.

The remainder of the paper is described as follows. In Sec. 2, a shape-based algorithm is proposed to identify a profile face. Section 3 presents an algorithm to detect a

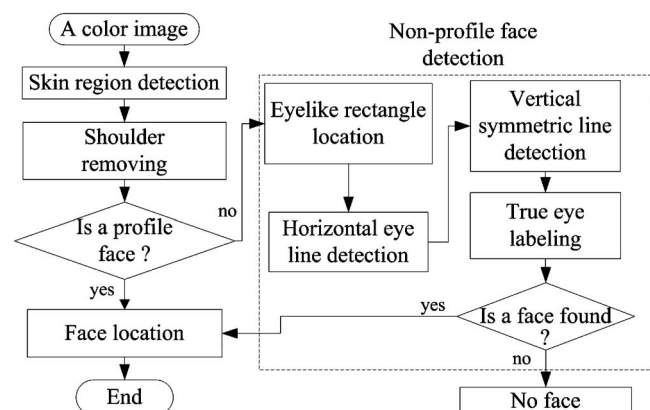


Fig. 1 Block diagram of the proposed face detector.

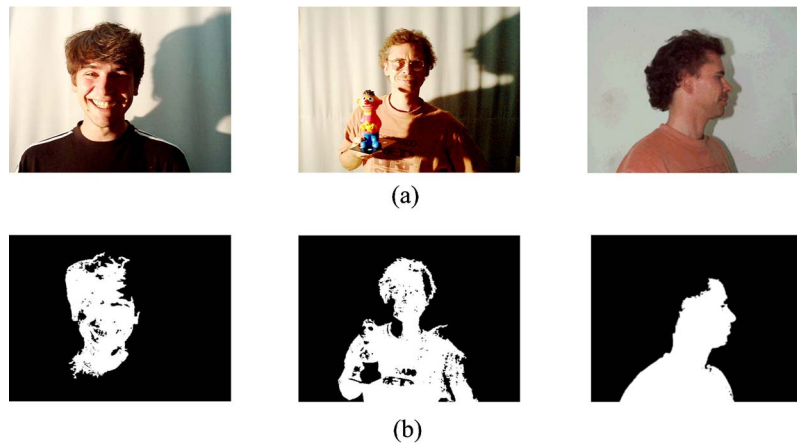


Fig. 2 Some results of applying Jing-Chen skin region extractor: (a) three images taken under various lighting environments and (b) The extracted skin regions (white pixels) using Jing-Chen skin region detector.

nonprofile face. In Sec. 4, some experimental results based on the HHI and Champion face databases are given to demonstrate the effectiveness of the proposed method. In Sec. 5, we present a conclusion.

2 Profile Detection

In this section, we provide a method to determine if an image contains a profile face. First, the skin region detector proposed by Jing and Chen¹² is adopted to extract skin regions from an input image. Figure 2 shows the extracted results from some face images with different poses taken

under various lighting environments. Note that some pixels in clothes with color similar to skin are also labeled as skin. In the following, we provide a method to remove these pixels.

2.1 Shoulder-Removing Procedure

Figure 3 shows an example of two men, one [in Fig. 3(a)] wears a T-shirt of skinlike color and the other [in Fig. 3(b)] wears a T-shirt of nonskin color. Figures 3(c) and 3(d) show the results of applying the Jing-Chen method to Figs. 3(a) and 3(b), respectively. In Fig. 3(c), pixels on the shoulder are labeled as skin pixels. Here, a projection-based procedure is provided to remove the shoulder part.

First, we need to determine whether a skin region includes a shoulder part. In general, the shoulder of a person is wider than the head and neck. On the basis of this fact, the horizontal projection of skin pixels is used to remove

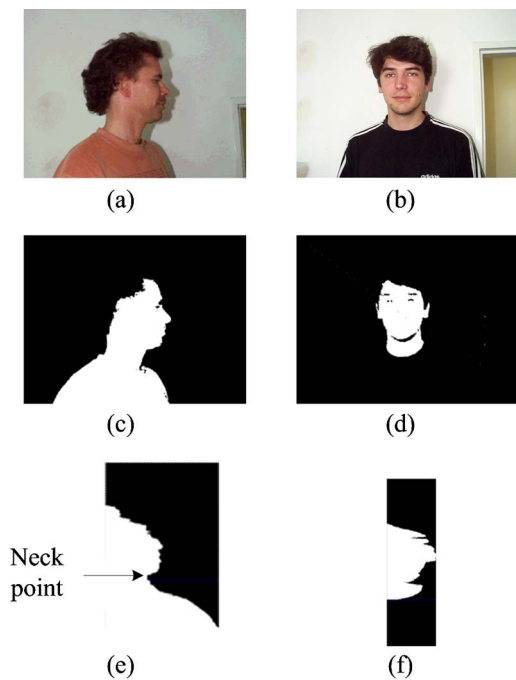


Fig. 3 Example showing two men wearing clothes with/without skinlike color: (a) man wearing a T-shirt of skinlike color, (b) man wearing a T-shirt of nonskinlike color, (c) detected skin region of (a), (d) detected skin region of (b), (e) horizontal projection of (c), and (f) horizontal projection of (d).

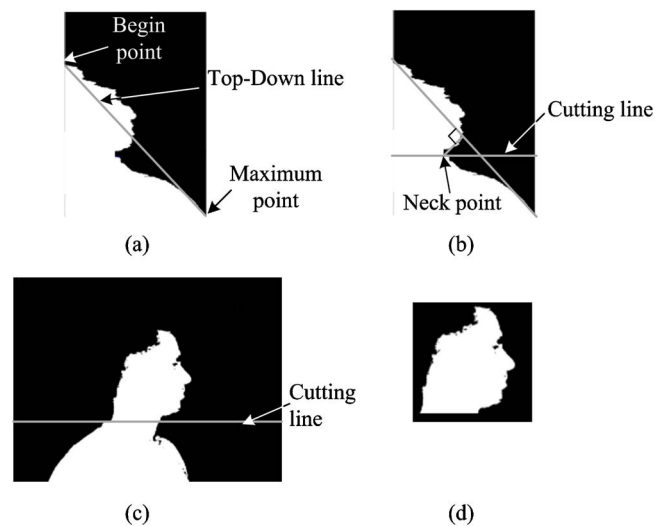


Fig. 4 Example for removing the shoulder from a skin region: (a) the Top-Down line for a projection histogram, (b) the neck point and the cutting line located, (c) the located cutting line on Fig. 3(c), and (d) result of removing shoulder from (c).

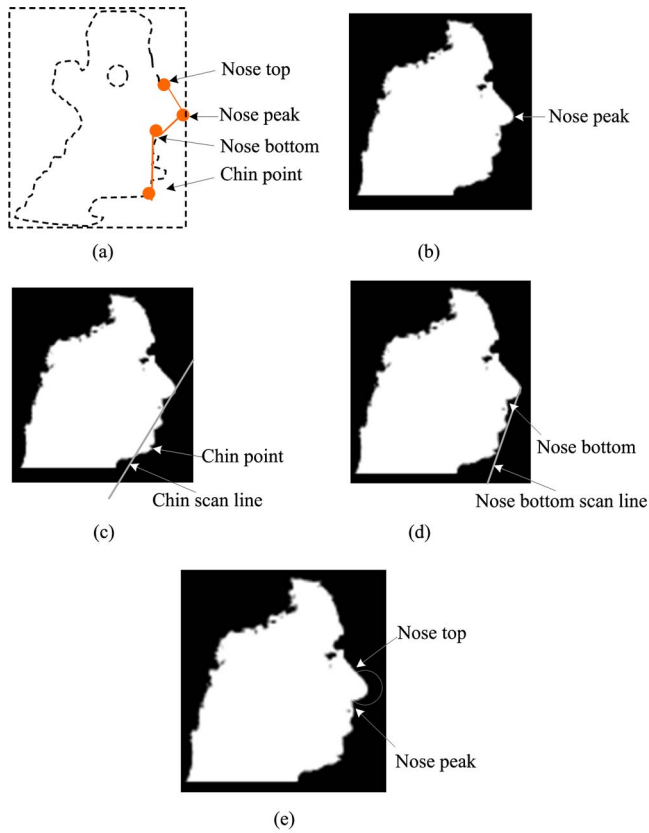


Fig. 5 Example for illustrating the profile features: (a) some feature points on a right profile, (b) extracted nose peak, (c) extracted chin scan line and chin point, (d) extracted nose bottom scan line and nose bottom, and (e) extracted nose top.

shoulder. Figures 3(e) and 3(f) show the horizontal projections of skin pixels in Figs. 3(c) and 3(d), respectively. From these figures, we can see that, if a shoulder exists, then the number of the labeled skin pixels below the middle part of the whole skin region, L , should be larger than that of the upper one, U . On the basis of this fact, $L/U > \sigma_s$ is applied to judge whether a skin region includes a shoulder part. In this paper, the threshold σ_s is 1.4.

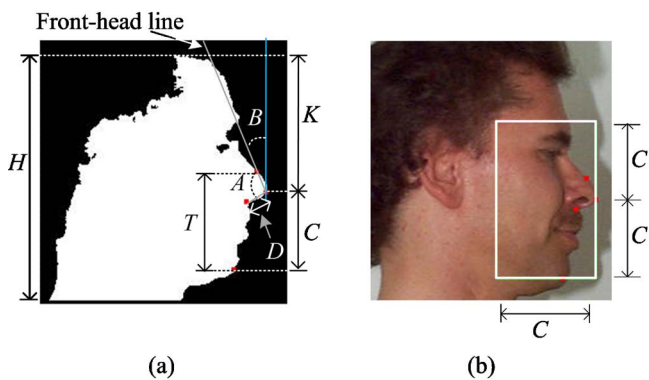


Fig. 6 Example to show the defined profile variables and the face rectangle: (a) the defined variables for a skin region and (b) the defined profile face rectangle.

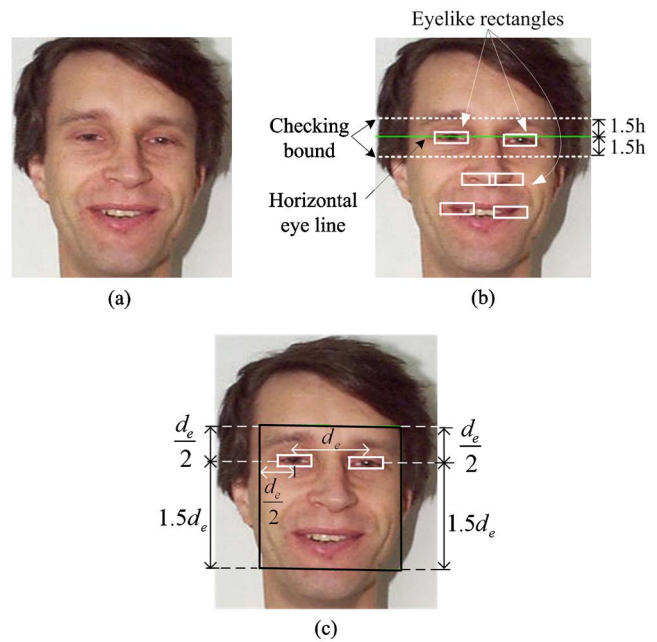


Fig. 7 Example for simple face model: (a) a face image, (b) the located horizontal eye line and ERs, and (c) the defined face eye rectangle.

If a skin region is determined to have a shoulder, then the neck location is considered as a good cutting point to remove the shoulder part. Because the neck is thinner than the other part of a human body, it will appear at the valley of the projection histogram [see Fig. 3(e)]. Thus, we take the valley point as the neck point. In order to locate the neck point, the beginning and maximum points of the projection histogram are used to form a base line called the Top-Down line [see Fig. 4(a)]. For each histogram point below the Top-Down line, we evaluate the distance from the histogram point to the Top-Down line. The point with maximum distance is considered the neck point [see Fig. 4(b)], and the horizontal line passing the neck point is considered the cutting line. Figure 4(c) shows the detected cutting line on a skin region. After locating the cutting line, all skin pixels below the cutting line are removed. Figure 4(d) shows the result of shoulder removal. Now, we decide if the remaining skin is a profile face. There are two kinds of profiles, one is a right profile; the other is a left profile. Because these two kinds of profiles have the same characteristics, in the following, we will only describe how to detect a right profile, as to left profiles, a similar way can be applied.

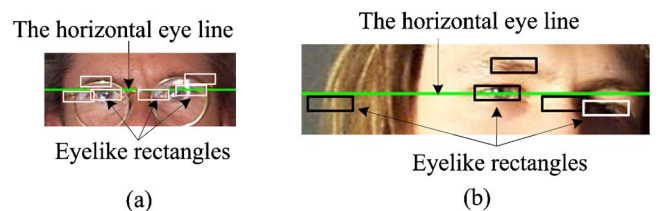


Fig. 8 Two examples for the complexity face model: (a) a man with glasses and (b) a man under bias lighting source.

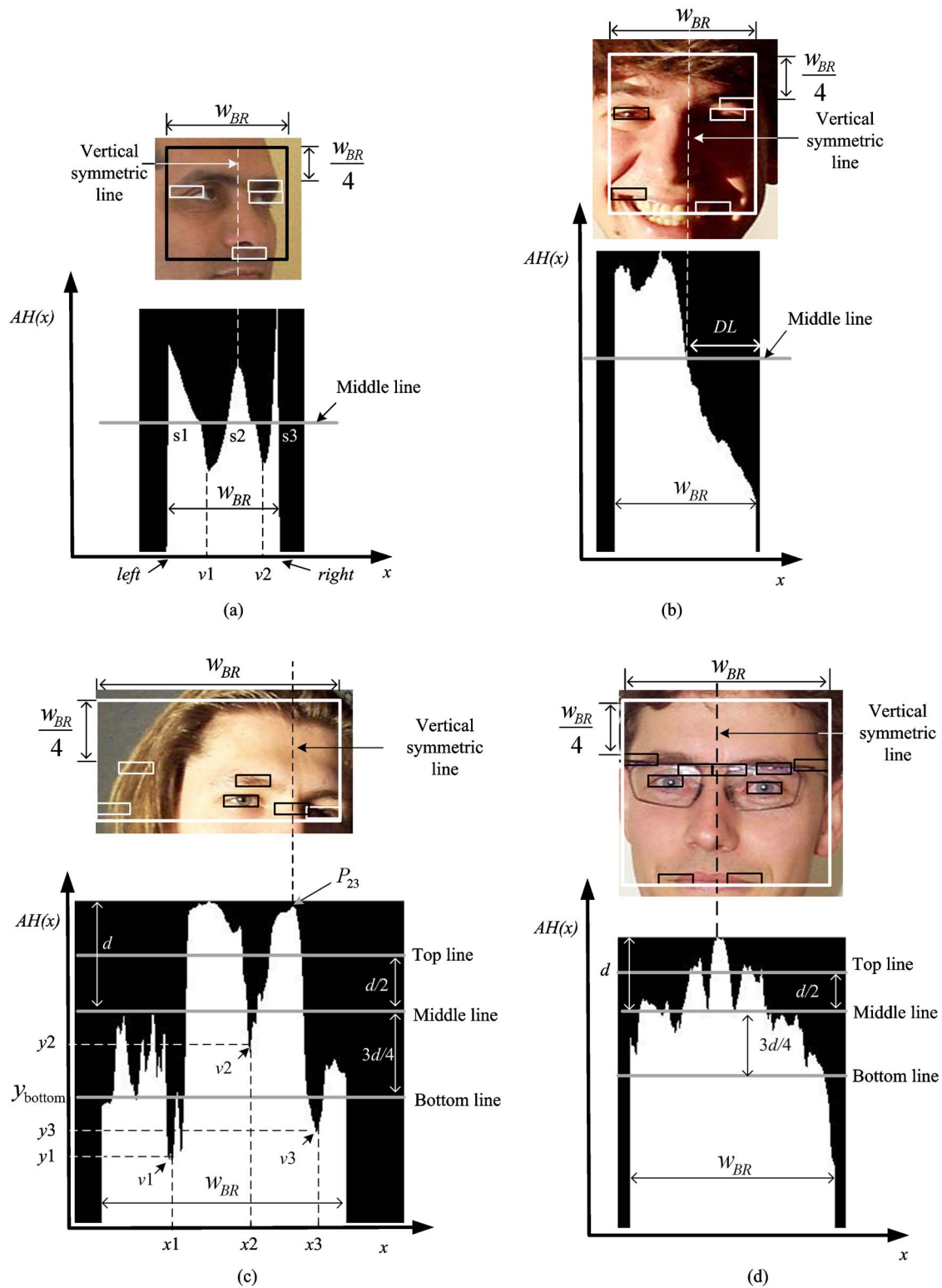


Fig. 9 Vertical histogram projection patterns and detected vertical symmetric lines: (a) half-profile pattern, (b) a bias lighting pattern, (c) a near frontal pattern with left-side pose, and (d) a normal pattern.

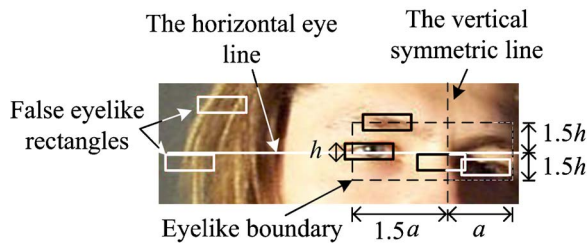


Fig. 10 Example to illustrate the eyelike boundary for a skin region.

2.2 Profile Feature Extraction

There are some feature points [see Fig. 5(a)] on a profile. These are nose peak, nose bottom, nose top, and chin point. On the basis of the geometric relations among these points, we can judge if a skin region is a profile. Here, we will provide a method to extract these points.

First, the furthest right point of a skin region is considered as the nose peak [see Fig. 5(b)]. Next, a vertical line V passing through the nose peak is taken. Line V is then rotated clockwise with respect to the nose peak until the length of the intersection segment between the rotated V and the skin region is larger than a predefined threshold. The rotated V is then defined as the chin scan line. For each contour pixel of the skin region below the nose peak and at the right side of the chin scan line, the distance from the pixel to the chin scan line is evaluated, and the point with the maximum distance is considered as the chin point [see Fig. 5(c)].

On the basis of the extracted chin point, the line from the nose peak to the chin point is defined as nose-bottom scan line, which will be used to locate the nose bottom. Following the contour points from the nose peak to the chin point, the contour point with the maximum distance to the nose-bottom scan line is considered as the nose bottom [see

Fig. 5(d)]. Finally, in order to locate the nose top, we draw a circle using the nose peak as its center and the distance from the nose bottom to the center as its radius; the top point of the skin region on the circle is considered as the nose top [see Fig. 5(e)]. On the basis of these extracted points, we will provide a procedure to check if a skin region is a profile.

Four rules are provided to verify the extracted profile features. At first, we define some profile variables. Let H be the height of the skin region, T be the vertical distance from the nose top to the chin point, C be the vertical distance from the nose peak to the chin point, D be the distance from the nose peak to the nose bottom, and K be the vertical distance from the nose peak to the top of the skin region. Define A to be the angle formed by the three points: nose top, nose peak, and nose bottom. In order to determine the front-head part of a profile face, we define a vertical line $V2$ passing through the nose peak and then rotated counterclockwise with respect to the nose peak until the length of the intersection segment between rotated $V2$ and the skin region is larger than a predefined threshold. The rotated $V2$ is then defined as the front-head line and B to be the angle between the front-head line and the vertical line passing through the nose peak. Figure 6(a) shows an example for the above-defined variables. On the basis of these variables, four rules for profile checking are given as follows:

Rule 1: $T > H/4$.

Rule 2: $D < 0.5 C$.

Rule 3: $0.85 K < C < 1.2 K$.

Rule 4: $45 < A < 150$ deg and $15 < B \leq 45$ deg.

If all rules are satisfied, the skin region is considered as a profile face.

If the skin region is not considered as a profile, the skin region is rotated according to the degree sequence $\{+5, -5, +10, -10, +15, -15\}$, and the profile detection proce-

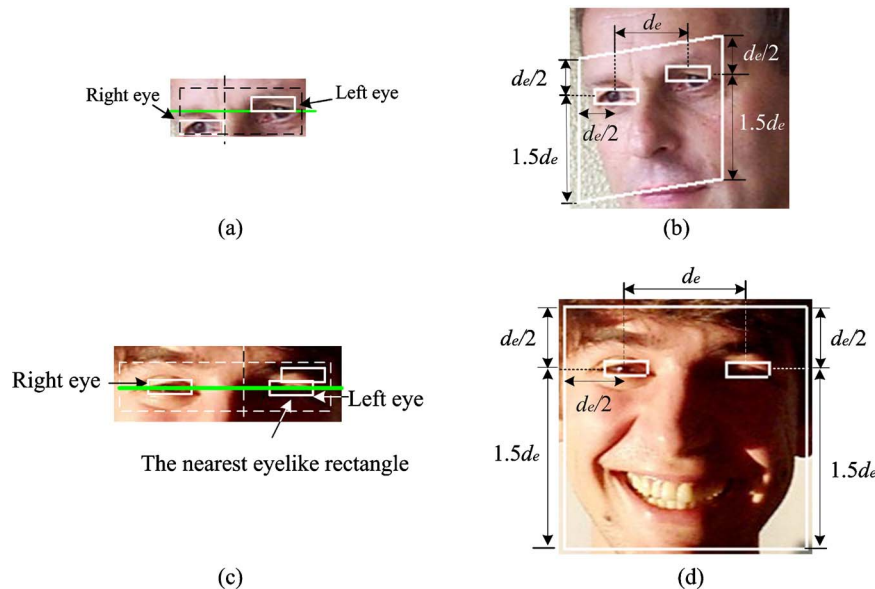


Fig. 11 Two examples for true eye and face location: (a) a case satisfying rule 1, (b) the detected face location based on the eye locations from (a), (c) a case satisfying rule 2, and (d) the detected face location based on the eye locations of (c).

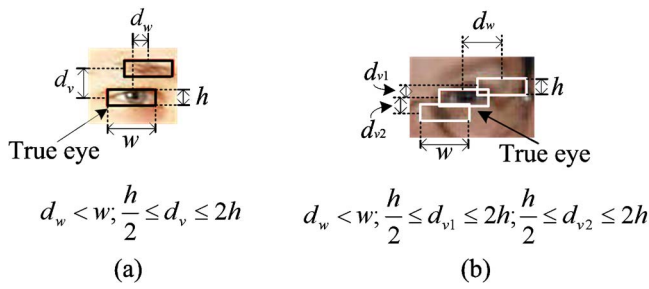


Fig. 12 Two examples for the two kinds of eye patterns: (a) two-layered pattern and (b) three-layered pattern.

cedure is applied again. On the basis of the nose peak and the distance C , a rectangle called a profile-face rectangle is formed and we use the rectangle to identify the profile-face location. Figure 6(b) shows an example of the detected face rectangle for a profile face.

3 Nonprofile Face Detection

For a skin region not determined as a profile face, a non-profile face-detection procedure is then applied. Jing and Chen¹² have proposed a method to locate the horizontal eye line and some eyelike rectangles on a skin image. Each eyelike rectangle has the same height, h . On the basis of the output of the Jing–Chen method, we provide a method to determine if a skin region is a nonprofile face. Figure 7 gives an example. Fig. 7(a) is a face image, and Fig. 7(b) shows the located horizontal eye line (in green) and some eyelike rectangles using Jing–Chen’s method on Fig. 7(a). On the basis of the located horizontal eye line, we can define a checking bound, which is formed by a pair of lines with distance $1.5h$ from the horizontal eye line, to remove those false eyelike rectangles. In Fig. 7(b), we can see that only two eyelike rectangles are in the defined checking bound and the horizontal eye line passes through these two eyelike rectangles. We classify this layout as simple face model. For a simple face model, the only two ERs within the checking bound are considered as the true eyes. Let d_e be the distance between the two eyes. A face rectangle is then defined as shown in Fig. 7(c). However, if a man wears glasses or a face is taken under a bias lighting source, then more than two ERs will exist in the checking bound (see Fig. 8). We classify these skin regions as a complex face model. In the following, we will introduce a vertical symmetric line locator to solve the complex face model.

3.1 Vertical Symmetric Line Location

In general, face is a nearly symmetric pattern, a symmetric vertical line exists. There are some methods^{13–15} based on this property to extract the symmetric vertical line. However, they may fail when a face is taken under a biased lighting environment or is not frontal. A human face is a 3-D object; different lighting sources and poses will make the symmetric line location difficult. In order to overcome these factors, we first classify the complex model into four patterns: half profile, bias lighting, near frontal, and normal (see Fig. 9). From our observation, we found that the nose peak and forehead areas always have higher lighting response than other facial regions. And the areas of eyebrows

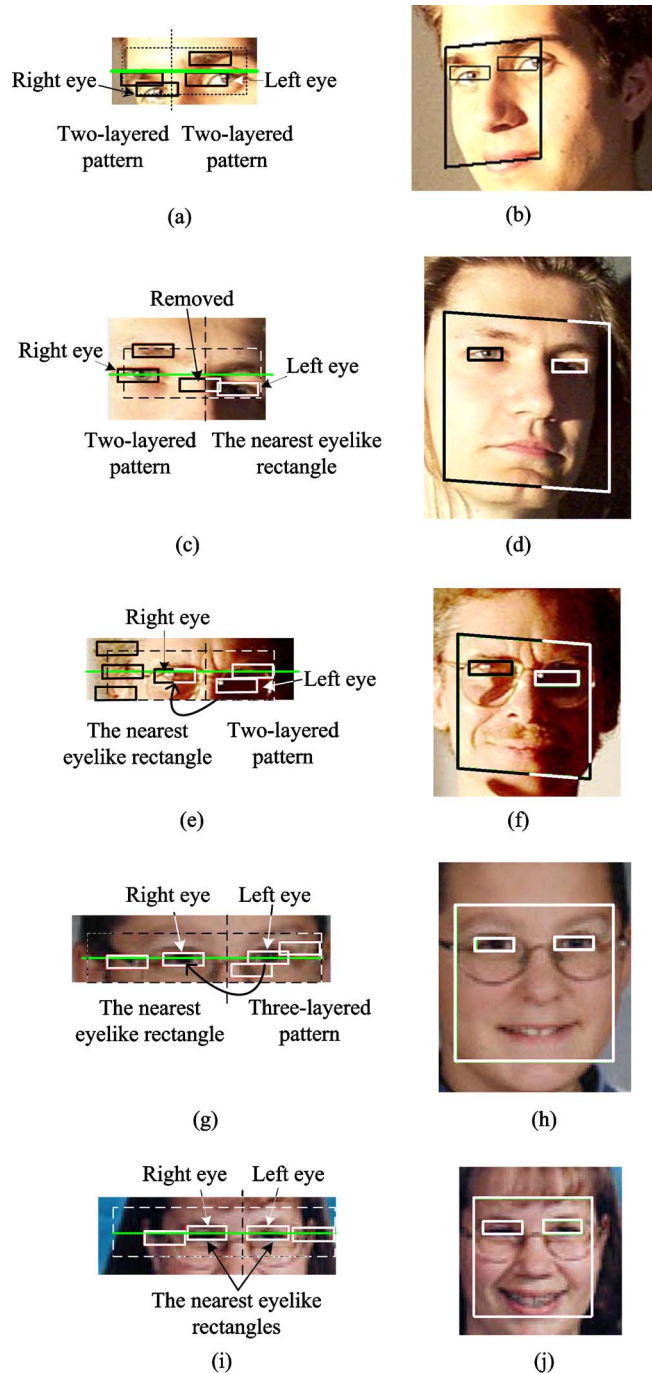


Fig. 13 Some examples for true eye and face rectangle location: (a) two-layered patterns at each side of the symmetric line, (b) the detected face location based on the true eye locations on (a), (c) one two-layered pattern detected, (d) the detected face location based on the eye locations on (c), (e) another example for only one two-layered pattern detected at one side, (f) the detected face location based on the eye locations on (e), (g) one three-layered pattern detected, (h) the detected face location based on the eye locations on (g), (i) example of other patterns detected, and (j) the detected face location based on the eye locations on (i).

and eyes contain fewer skin color pixels and have lower gray values than other facial regions. On the basis of these facts, we define a vertical skin projection histogram $AH(x)$ in Eq. (1) to catch these characteristics. Note that the pro-



Fig. 14 Part of the images from the HHI face database.

jection area, A , used in Eq. (1) is formed by extending BR $(1/4)w_{BR}$ height [see the black rectangle in Fig. 9(a)], where BR is the rectangle bounding all eyelike rectangles and w_{BR} is the width of BR. Figure 9 shows some projection results from some face images taken under different poses and lighting conditions

$$AH(x) = \sum_{(x,y) \in A} [\text{gray}(x,y) + Cr(x,y)]. \quad (1)$$

On the basis of the vertical projection histogram, we can do the classification and then locate the vertical symmetric

line. First, define $y_{\text{mid}} = 1 / w_{BR} \sum_{x=\text{left}}^{\text{right}} AH(x)$ to be the middle line of the histogram, where w_{BR} is the width of the projection area and “left” and “right” indicate the left and right bounds of the projection area. If there are only two valleys below the middle line [see Fig. 9(a)], and the intersection between the middle line and the histogram contains three segments, then we say this is a half profile, and the vertical line passing the peak between two valleys is considered the symmetric line [see Fig. 9(a)]. If the skin region is not a half profile, then bias lighting testing is conducted. In order to judge the shadow ratio on a face, we collect all dark



Fig. 15 Part of the images from the Champion face database.

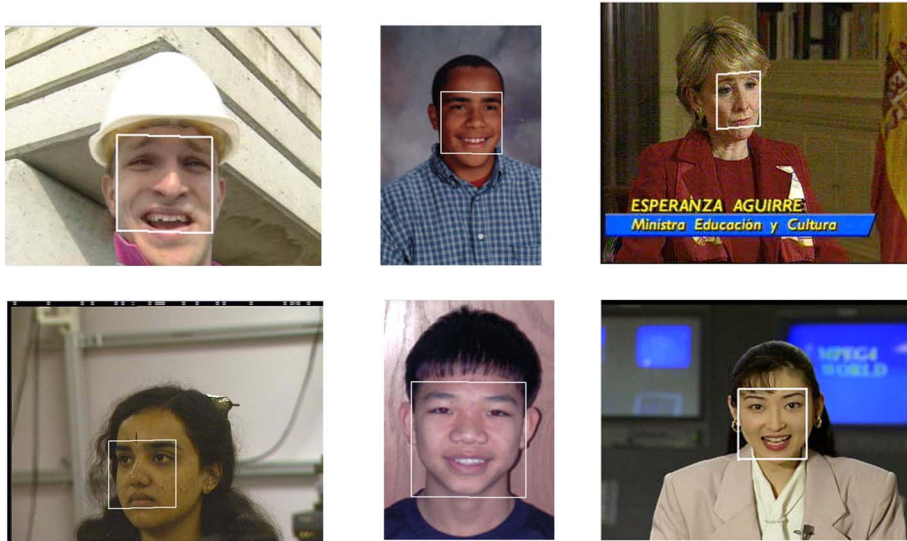


Fig. 16 Detection results for persons with different skin colors.

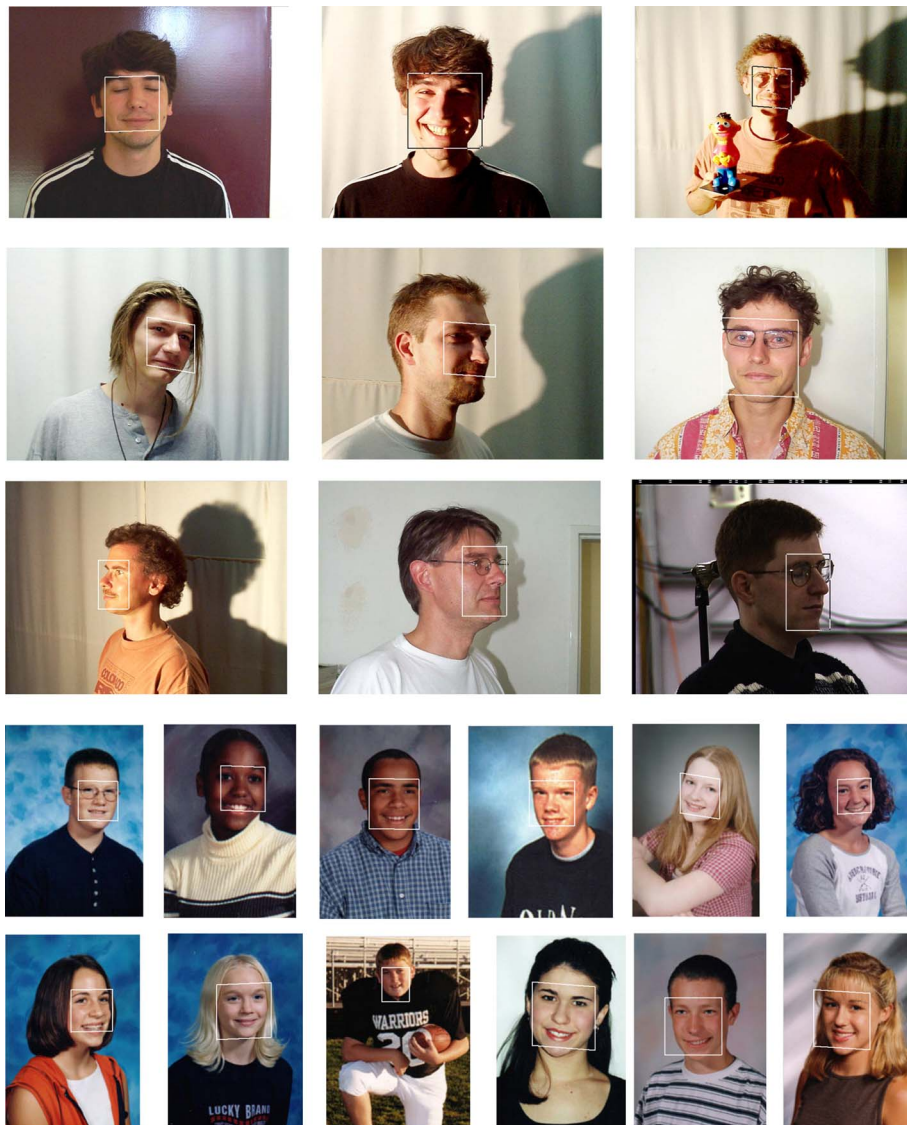


Fig. 17 The detection results for persons with different poses.

Table 1 Detection results on HHI database (image size 640 × 480).

Head pose		Frontal	Near frontal	Half profile	Profile	Total
No. of images		66	54	75	11	206
Face Detection						
No. of false positive	Proposed method	5	1	6	0	12
	Hsu et al. ⁵	4	6	14	3	17
Correct detection rate (%)	Proposed method	92.4	98.1	92	90.9	93.68
	Hsu et al. ⁵	89.4	90.71	74.67	18.18	80.58
Average execution time per image (s)	Proposed method	7.5 (on the mobile processor 1.4-GHz CPU)				
	Hsu et al. ⁵	22.97 (on the 1.7-GHz CPU)				

segments on the middle line. Let D_L be the longest dark segment [see Fig. 9(b)]. If the length of D_L is larger than $[(w_{BR}/2) - \sigma]$, we call this as a bias lighting pattern, and the vertical line passing the end point of D_L near the histogram middle side is considered as the symmetric line [see Fig. 9(b)]. In this paper, we set the threshold σ as $w_{BR}/8$. If the skin region is neither a half profile nor a bias lighting pattern, then we apply the near-frontal testing procedure. There are two kinds of near-frontal patterns; one is a face with left-side pose, and the other with right-side pose. In the following procedure, we describe how to test a left-side near-frontal pattern. Using a similar method, we can test right-side near-frontal patterns. At first, define two reference lines, $y_{top} = y_{mid} + d/2$ as the top line and $y_{bottom} = y_{mid} - 3d/4$ as the bottom line, where d is the distance from the global maximum peak of the histogram to the middle line. If there exists three valleys $v1 = (x_1, y_1)$, $v2 = (x_2, y_2)$, and $v3 = (x_3, y_3)$ satisfying the left-side rule as follows:

The left-side rule:

$$x_1 < x_2 < x_3,$$

$$t_1|x_2 - x_3| < |x_2 - x_1|,$$

$$|x_1 - x_3| > \frac{w_{BR}}{2} \quad \text{and} \quad y_1 < y_{bottom},$$

and the peak, $P_{2,3}$, between $v2$ and $v3$ is higher than y_{top} . Then, we consider the skin region to be a left-side near frontal face pattern and the vertical line passing $P_{2,3}$ as the symmetric line. Figure 9(c) shows an example of a man with left-side near-frontal face pattern. In this paper, t_1 is set as 1.2. Finally, for a skin region not belonging to any of the above three patterns, the vertical line passing the maximum peak not near the boundary of the projection area is considered the symmetric face line [see Fig. 9(d)].

3.2 False ER Removing

As we know, a pair of human eyes is symmetrically located on the left and right sides of the symmetric line of a face. That is, if we label one eye from a side of the symmetric line, then the other eye must locate at the other side and be symmetric to the labeled eye with respect to the symmetric line. Using this property, those false ER can be eliminated. On the basis of the vertical symmetric line, an eyelike boundary is defined to remove those false ERs. First, for each ER, evaluate the distance of the rectangle to the symmetric line. Second, the two farthest ER at both sides of the symmetric line are taken, and let a be the distance of the near one. Finally, based on the horizontal eye line and the ER height (h), we can define the eyelike boundary as shown in Fig. 10. Any ER out of the eyelike boundary is considered a false ER and is removed. Now, we will locate the true eyes from the remaining ERs.

Table 2 Detection results on Champion database (image size ~150 × 220).

	Proposed method	Hsu
No. of images	227	
No of false positive	7	14
Correct detection rate (%)	95.15	91.63
Average execution time per image (s)	4 (on the mobile processor 1.4-GHz CPU)	5.78 (on the 1.7-GHz CPU)

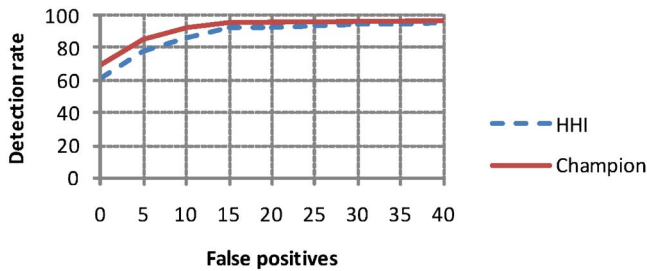


Fig. 18 ROC curves for our face detector on the HHI and Champion databases.

Table 3 Detection results on non-profile faces of HHI database.

	Proposed method	Chow
No. of images (nonprofile faces)	195 (206-11)	151 (selected)
No. of false positive	12	4
Correct detection rate (%)	93.8	92.7

3.3 True Eye-Locating Procedure

Yow and Cipolla¹⁶ use some geometric constraints to detect feature points, including two eye points; however, when a face picture is taken under a biased lighting condition, these feature points cannot be correctly detected. Here, a two-step procedure is designed to locate two true eyes. In the first step, two rules are provided to identify the true eyes. With located eye centers (lx_e, ly_e) and (rx_e, ry_e) , a parallelogram with the top-left point $(lx_e - d_e/2, ly_e - d_e/2)$ and bottom-right point $(rx_e + d_e/2, ry_e + 1.5d_e)$ is then defined to be face area [see Figs. 11(b) and 11(d)], where d_e is the horizontal distance between the two eyes. In order to include the mouth area, if the distance d_e is shorter than a threshold $1.2w$, then the bottom-right point of the face area is refined as $(rx_e + d_e/2, ry_e + 2d_e)$.

Rule 1: If exactly one ER locates at each side of the

symmetric line, these two ER are considered as the true eyes and the face rectangle is located [see Figs. 11(a) and 11(b)].

Rule 2: If only one ER locates at one side of the symmetric line and more than one at the other side, consider the only the ER as one true eye and identify the nearest ER on the other side as the other true eye. Figure 11(c) and 11(d) show an example of the located true eyes and the corresponding face location.

For those cases not satisfying rules 1 or 2, the second step is conducted. On the basis of the relative locations among eyebrows, glasses, and eyes, for the ER height (h) and width (w), two kinds of eye patterns (two layered and three layered) are defined to help locate true eyes.

Definition 1. A pair of two ER is called a two-layered pattern, if these two ER have horizontal distance d_w with

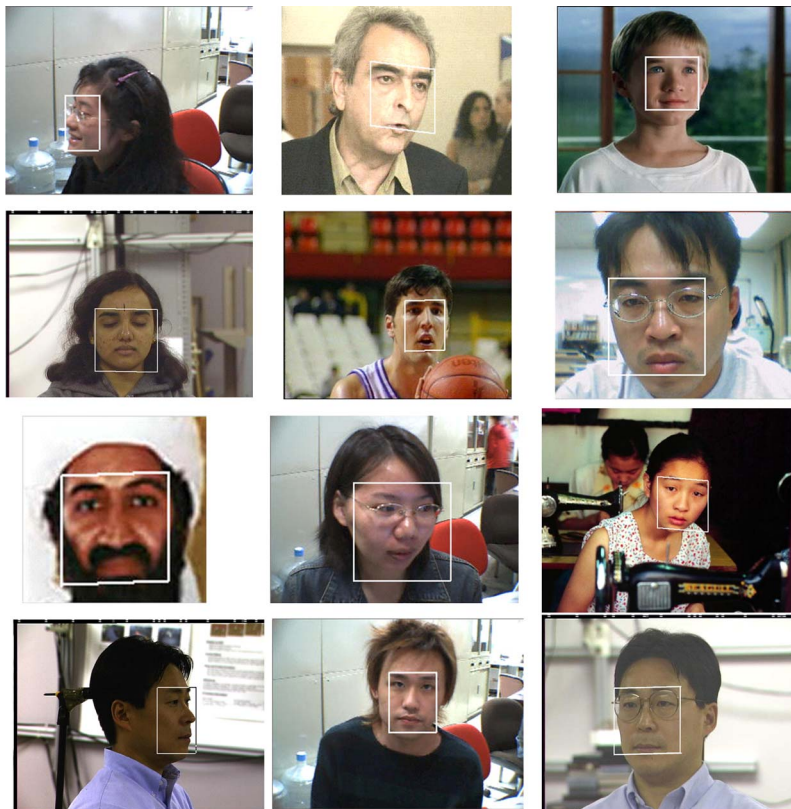


Fig. 19 The detection results of face images collected from our laboratory, the Internet, and MPEG7 video clips.



Fig. 20 The detection results for multiple faces.

$d_w < w$ and vertical distance d_v with d_v in $(h/2, 2h)$ [see Fig. 12(a)].

Definition 2. A group of three ER (R1, R2, R3) is called a three-layered pattern if the horizontal distance between any two neighboring rectangles is less than w and the vertical distance is $(h/2, 2h)$. Figure 12(b) gives an example of the three-layered pattern.

In the second step, if we find a pair of two-layered patterns located at each side of the symmetric line, respectively, then both bottom rectangles are identified as the true eyes [see Figs. 13(a) and 13(b)]. If there is only one two-layered pattern detected, then we choose the bottom ER as the true eye and remove all ER that intersect with the vertical symmetric line. The nearest ER on the other side of the symmetric line is considered the other eye. Figure 13(c) and 13(e) show two examples of this case. If there is no two-layered eye pattern on any side, then we consider three-layered patterns. For a three-layered eye pattern, the middle rectangle is identified as the true eye. If a three-layered pattern is detected on one side, then the other eye is identified to be the closest ER on the other side. Figure 13(g) shows an example of this case. If there are neither of the two kinds of patterns, then we consider the nearest rectangles to the symmetric and horizontal lines as the true eyes [see Fig. 13(i)].

4 Experimental Results

In order to show the effectiveness of the proposed method, we apply the method to the HHI face database¹⁷ of 206 images (see Fig. 14) and the Champion face database¹⁸ of 227 images (see Fig. 15). We also collect some images from our laboratory, the Internet, and MPEG7 video clips to evaluate the performance. These contain images of people of different race under different kinds of lighting conditions (such as overhead, side, and color lighting) and poses. The size of faces ranges from 252×229 to 79×79 . Figure 16 shows the successful results of applying our method to some faces with different skin color. The successful results for faces with different poses and eyeglasses are shown in Fig. 17. Even if there is a shadow on a face, the face can also be detected.

In this paper, if the located face rectangle bounds a face, we consider it a correct detection. If a face rectangle is found for a nonface region, we call it a false-positive detection. For the HHI database, the correct detection rate is 93.68% and, for the Champion database, it is 95.15%. Tables 1 and 2 show the detail detection results for both

databases. Table 3 shows the detection result of the nonprofile faces in HHI. In order to show the effectiveness of the proposed method, the original results of Hsu et al.⁵ using both databases and Chow et al.⁶ for HHI database are also given in Tables 1–3 to do comparisons.

The receiver operating characteristic (ROC) curves for both databases are also given in Fig. 18. Figure 19 shows the successful detection results for a set of images from our laboratory, the Internet, and MPEG7 video clips. Figure 20 shows detection results of multiple faces.

5 Conclusion

In this paper, we have developed a face detector for face images under various environments and poses. On the basis of the proposed method, we can handle a left/right profile face and a nonprofile face. In addition, we also present an efficient procedure to determine if a person wears skinlike-color clothes and output the neck point as a cutting point to separate the head and shoulder part of the body for further processing. In order to handle the environments and pose variations, the detector combines the shape, color, and lighting distribution information to locate true eyes, and then, to locate the face location. Experimental results show that the proposed method is robust over a wide range of lighting conditions, various poses, and race. Even is there is a closed eye on a face, the face can also be detected. The proposed face detector has a higher correct detection rate than those of Hsu et al.⁵ and Chow et al.⁶

Acknowledgment

This research was supported in part by the National Science Council of R.O.C. under Contract No. NSC-97-2221-E-009-137.

References

1. M. H. Yang, D. J. Kriegman, and N. Ahuja, "Detecting faces in images: a survey," *IEEE Trans. Pattern Anal. Mach. Intell.* **24**(1), 34–58 (2002).
2. M. Turk and A. Pentland, "Eigenfaces for recognition," *J. Cognit. Neurosci.* **3**(1), 71–86 (1991).
3. H. Rowley, S. Baluja, and T. Kanade, "Neural network-based face detection," *IEEE Trans. Pattern Anal. Mach. Intell.* **20**(1), 23–38 (1998).
4. C. A. Waring and X. Liu, "Face detection using spectral histograms and SVMs," *IEEE Trans. Syst., Man, Cybern., Part B: Cybern.* **35**(3), 467–476 (2005).
5. R. L. Hsu, M. A. Mottaleb, and A. K. Jain, "Face detection in color images," *IEEE Trans. Pattern Anal. Mach. Intell.* **24**(5), 696–706 (2002).

6. T. Y. Chow, K. M. Lam, and K. W. Wong, "Efficient color face detection algorithm under different lighting conditions," *J. Electron. Imaging* **15**(1), 013015(1)–013015(10) (2006).
7. F. Y. Shih and C. F. Chuang, "Automatic extraction of head and face boundaries and facial features," *Inf. Sci. (N.Y.)* **158**, 117–130 (2004).
8. J. Wu and Z. Zhou, "Efficient face candidates selector for face detection," *Pattern Recogn.* **36**(5), 1175–1186 (2003).
9. J. Miao, B. Yin, K. Wang, L. Shen, and X. Chen, "A hierarchical multiscale and multiangle system for human face detection in a complex background using gravity-center template," *Pattern Recogn.* **32**(7), 1237–1248 (1999).
10. J. Song, Z. Chi, and J. Liu, "A robust eye detection method using combined binary edge and intensity information," *Pattern Recogn.* **39**(6), 1110–1125 (2006).
11. V. Perlibakas, "Automatic detection of face features and exact face contour," *Pattern Recogn. Lett.* **24**(16), 2977–2985 (2003).
12. M. Q. Jing and L. H. Chen, "A novel method for horizontal eye line detection under various environments," *Int. J. Pattern Recognit. Artif. Intell.* (to be published).
13. X. Chen, P. J. Rynn, and K. W. Bowyer, "Fully automated facial symmetry axis detection in frontal color images," in *4th IEEE Workshop on Automatic Identification Advanced Technologies*, pp. 106–111, (2005).
14. N. Nakao, W. Ohyama, T. Wakabayashi, and F. Kimura, "Automatic detection of facial midline and its contributions to facial feature extraction," *Electron. Lett. Comput. Vis. Image Anal* **6**(3), 55–65 (2008).
15. H. J. So, M. H. Kim, Y. S. Chung, and N. C. Kim, "Face detection using sketch operators and vertical symmetry," *Lect. Notes Comput. Sci.* **4027**, 541–551 (2006).
16. K. C. Yow and R. Cipolla, "Feature-based human face detection," CUED/F-INFENG/TR 249, University of Cambridge, Department of Engineering, England (Aug. 1996).
17. MPEG7 Content Set from Heinrich Hertz Institute, (<http://www.darmstadt.gmd.de/mobile/hm/projects/MPEG7/Documents/N2466.html>) (Oct. 1998).
18. The Champion Database, (http://www.libfind.unl.edu/alumni/events/breakfast_for_champions.htm) (Mar. 2001).



Min-Quan Jing received his BS in computer science engineering from Chung Hua University, Hsinchu, Taiwan, in 1997, and MS in computer and information science from National Chiao Tung University in 1999, where he is working on his PhD at the Institute of Computer Science. His current research interests include image processing and face recognition.



Ling-Hwei Chen received her BS in mathematics and MS in applied mathematics from National Tsing Hua University, Hsinchu, Taiwan in 1975 and 1977, respectively, and PhD in computer engineering from National Chiao Tung University, Hsinchu, Taiwan, in 1987. From 1977 to 1979 she worked as a research assistant in the Chung-Shan Institute of Science and Technology, Taoyan, Taiwan, then became a research associate in the Electronic Research

and Service Organization, Industry Technology Research Institute, Hsinchu, Taiwan. From 1981 to 1983, she worked as an engineer in the Institute of Information Industry, Taipei, Taiwan. She is now a professor in the Department of Computer Science at the National Chiao Tung University. Her research interests include image processing, pattern recognition, video compression, and multimedia steganography.